Resource Allocation in NOMA-Enhanced Backscatter Communication Networks for Wireless Powered IoT

Gang Yang, *Member, IEEE*, Xinyue Xu, and Ying-Chang Liang, *Fellow, IEEE*

***Abstract*—This letter considers a non-orthogonal-multiple-access (NOMA)-enhanced bistatic backscatter communication network where multiple backscatter devices (BDs) transmit to a backscatter receiver using a protocol integrating NOMA with dynamic time-division-multiple-access. We maximize the minimum throughput among all BDs by jointly optimizing the BDs' backscatter time and power reflection coefficients, subject to the BDs' harvested energy constraints and other constraints. By applying the block coordinated decent and successive convex optimization techniques, an efficient iterative algorithm is proposed to find a sub-optimal solution to the formulated non-convex problem. Numerical results show that the proposed scheme achieves significant throughput gain compared to the benchmark scheme.**

***Index Terms*—Backscatter communication, non-orthogonal multiple access, wireless powered communication, throughput optimization, Internet-of-Things.**

I. Introduction

BACKSCATTER communication (BackCom), which enables passive backscatter devices (BDs) to modulate their information over incident sinusoidal carriers or ambient radio-frequency (RF) carriers without using power-hungry and costly RF transmitter, is an energy- and cost-efficient communication technology for Internet-of-Things (IoT) [1]–[5]. Traditional BackCom systems like radio frequency identification adopt monostatic architecture with co-located carrier transmitter (CT) and backscatter receiver (BR), and the communication coverage is inherently limited by the short distance of energy transfer to passive BDs like tags, due to exponential decaying of electromagnetic waves with respect to distance. A bistatic architecture with spatially separated CT and BR can extend the coverage significantly [2]. By deploying the CT closer to the BD, the BD was demonstrated to harvest sufficient energy and communicate with a remote BR several hundred meters away [1], [2].

Manuscript received August 17, 2019; revised September 19, 2019; accepted September 23, 2019. Date of publication September 27, 2019; date of current version January 9, 2020. This work was supported by the National Natural Science Foundation of China under Grant 61601100 and Grant U1801261. The associate editor coordinating the review of this article and approving it for publication was X. Chu. *(Corresponding author: Ying-Chang Liang.)*

G. Yang and X. Xu are with the National Key Laboratory of Science and Technology on Communications, University of Electronic Science and Technology of China, Chengdu 611731, China, and also with the Center for Intelligent Networking and Communications, University of Electronic Science and Technology of China, Chengdu 611731, China (e-mail: yanggang@uestc.edu.cn; 201821220447@std.uestc.edu.cn).

Y.-C. Liang is with the Center for Intelligent Networking and Communications, University of Electronic Science and Technology of China, Chengdu 611731, China (e-mail: liangyc@ieee.org).

Digital Object Identifier 10.1109/LWC.2019.2944369

To support massive IoT devices in 5G and beyond systems, non-orthogonal multiple access (NOMA) that serves multiple users in the same time-frequency resource is appealing due to its high spectrum efficiency [6]. Moreover, NOMA-enhanced BackCom is recently recognized as a promising spectrum-, energy-, and cost-efficient technology for collecting massive low-power IoT devices [7]–[11]. In [7], the authors proposed a novel symbiotic system which integrates NOMA and ambient BackCom [8]–[10], and analyzed the outage and ergotic rate performances. The authors in [11] considered a NOMA-enhanced monostatic BackCom system, and analyzed the average number of successfully decoded bits. To our best of knowledge, there is no existing work focusing on performance optimization for a NOMA-enhanced bistatic BackCom network (BBCN).

In this letter, we study the resource allocation problem for a NOMA-enhanced BBCN in which multiple single-antenna BDs receive carrier (also energy) signals from a CT and transmit to a multi-antenna BR. A transmission protocol integrating NOMA with dynamic time-division-multiple-access (TDMA) is proposed to enhance spectrum efficiency and exploit channel dynamics. The aim is to maximize the minimum throughput among all BDs by jointly optimizing the BDs' backscatter time and power reflection coefficients, subject to the BDs' harvested energy constraints, signal-to-interference-plus-noise-ratio (SINR) constraints and other practical constraints. By applying the block coordinated decent and successive convex optimization techniques, an efficient iterative algorithm is proposed to find a sub-optimal solution to the formulated non-convex problem. Numerical results show that the proposed scheme achieves significant throughput gain compared to the benchmark scheme of traditional orthogonal-multiple-access (OMA) with dynamic TDMA.

II. System Model and Problem Formulation

As shown in Fig. 1, this letter considers a NOMA-enhanced BBCN which consists of a CT, multiple single-antenna BDs, and a BR equipped with R ($R \geq 1$) antennas. The CT transmits sinusoidal carrier signals, and each BD modulates its information symbols over incident carriers by intelligently changing its load impedance. The BR receives the signals and recovers the information from all BDs.

We propose a frame-based transmission protocol which integrates M-BD NOMA multiplexing and dynamic TDMA with K transmission slots, with $M \geq 1$ and $K \geq 1$. Each frame consists of a training phase with MK training slots and a transmission phase. In each training slot, only one BD

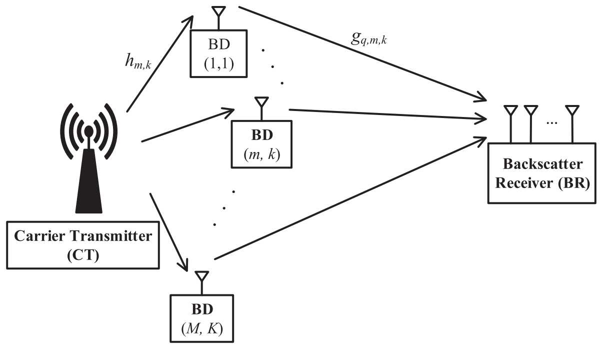

Fig. 1. System description for a BBCN.

backscatters carrier signals with the same power reflection coefficient, with all other BDs keeping silent, and the BR estimates the BD's channel. The BDs are sorted decreasingly based on the BR's received power levels, and categorized into *M* power groups sequentially. In each transmission slot with duration $\tau_k \in [0, 1]$, for $k = 1, \ldots, K$, the BR selects one BD from each group to perform NOMA transmission, following existing pairing schemes [12], [13]. The transmission phase is normalized to one, implying $\sum_{k=1}^{K} \tau_k = 1$. Denote $\boldsymbol{\tau} = [\tau_1, \ldots, \tau_K]$.

The block flat-fading channel model is considered, and the block length is longer than the frame duration. As shown in Fig. 1, we use $h_{m,k}$ to denote the channel coefficient between the CT and the BD selected from the *m*th power group in the *k*th slot, denoted as BD (*m, k*), for $m = 1, \ldots, M$, $g_{r,m,k}$ to denote the channel coefficient between BD (*m, k*) and the *r*th antenna of the BR. Denote $\mathbf{h}_k = [h_{1,k} \ \ldots \ h_{M,k}]^T$, $\mathbf{g}_{m,k} = [g_{1,m,k} \ \cdots \ g_{R,m,k}]^T$, and let $\mathbf{f}_{m,k} = h_{m,k}\mathbf{g}_{m,k}$. All channels are assumed to be mutually independent[1] and perfectly estimated by the BR.

Let P_t be the CT's transmit power, and $s_{m,k}(n)$ be the information symbol of each BD (*m,k*) which is assumed to follow the circularly symmetric complex Gaussian (CSCG) distribution with unit power [14]. Denote the power reflection coefficient of BD (*m, k*) as $\omega_{m,k} \in [0, 1]$ [15],[2] and the corresponding matrix as $\mathbf{\Omega}$. Its backscattered signal is thus $x_{m,k}(n) = \sqrt{P_t \omega_{m,k}} s_{m,k}(n) h_{m,k}$. Denote the energy conversion efficiency as $\epsilon_{m,k} \in (0, 1)$. The energy harvested by BD (m, k) is thus

$$\begin{aligned} E_{m,k} &= \epsilon_{m,k} P_t \left[\tau_k |h_{m,k}|^2 (1 - \omega_{m,k}) + (1 - \tau_k) |h_{m,k}|^2 \right] \\ &= \epsilon_{m,k} P_t |h_{m,k}|^2 (1 - \tau_k \omega_{m,k}). \end{aligned} \tag{1}$$

The signal received at the BR in the *k*th slot is

$$\mathbf{y}_k(n) = \sum_{m=1}^{M} \mathbf{f}_{m,k} \sqrt{P_t \omega_{m,k}} s_{m,k}(n) + \mathbf{z}(n), \tag{2}$$

[1]In practice, the BDs' scattering environments are typically independent, and the minimum inter-antenna distance of the BR is typically longer than the half wavelength of the transmitted electromagnetic wave.

[2]Due to the energy conservation law and one-to-one mapping from complex signal constellation point to $\omega_{m,k}$ [14], the $\omega_{m,k}$ can approximate a continuous value between 0 and 1, for practical BackCom systems with higher quadrature amplitude modulation like those in [15].

where the CSCG noise vector $\mathbf{z}(n) \sim \mathcal{CN}(\mathbf{0}, \sigma^2 \mathbf{I}_R)$. The noise $\mathbf{z}(n)$ is assumed to be independent of $s_{m,k}(n)$'s.

Let $\rho = \frac{P_t}{\sigma^2}$. The BR adopts the maximal-ratio-combining (MRC) detector $\mathbf{u}_{m,k} = \frac{\mathbf{f}_{m,k}^*}{\|\mathbf{f}_{m,k}\|}$ to decode the signal from the BD (*m, k*), as $\widehat{s}_{m,k}(n) = \mathbf{u}_{m,k}^T \mathbf{y}_k(n)$. Assuming that the BR decodes the signals from the BDs with indexes from (1, *k*) to (*m* −1, *k*) successfully, the throughput of BD (*m, k*) is obtained as

$$C_{m,k} = \tau_k \log_2 \left(1 + \frac{\rho \|\mathbf{f}_{m,k}\|^4 \omega_{m,k}}{\sum_{i=m+1}^{M} \rho |\mathbf{f}_{m,k}^H \mathbf{f}_{i,k}|^2 \omega_{i,k} + \|\mathbf{f}_{m,k}\|^2} \right). \tag{3}$$

To ensure throughput fairness among BDs, we maximize the minimum throughput among all BDs by jointly optimizing the BDs' backscatter time allocation $\boldsymbol{\tau}$ and power reflection coefficients $\mathbf{\Omega}$. The problem is formulated as

$$\text{(P1)}: \max_{\boldsymbol{\tau}, \mathbf{\Omega}, Q} \quad Q \tag{4a}$$

$$\text{s.t.} \quad \tau_k \log_2 \left(1 + \frac{\rho \|\mathbf{f}_{m,k}\|^4 \omega_{m,k}}{\sum_{i=m+1}^{M} \rho |\mathbf{f}_{m,k}^H \mathbf{f}_{i,k}|^2 \omega_{i,k} + \|\mathbf{f}_{m,k}\|^2} \right) \geq Q, \quad \forall m, k \tag{4b}$$

$$\frac{\rho \|\mathbf{f}_{m,k}\|^4 \omega_{m,k}}{\sum_{i=m+1}^{M} \rho |\mathbf{f}_{m,k}^H \mathbf{f}_{i,k}|^2 \omega_{i,k} + \|\mathbf{f}_{m,k}\|^2} \geq \lambda, \quad \forall m, k \tag{4c}$$

$$\epsilon_{m,k} P_t |h_{m,k}|^2 (1 - \tau_k \omega_{m,k}) \geq E_{\mathsf{min}}, \forall m, k \tag{4d}$$

$$0 \leq \omega_{m,k} \leq 1, \forall m, k \tag{4e}$$

$$\sum_{k=1}^{K} \tau_k \leq 1 \tag{4f}$$

$$\tau_k \geq 0, \forall k. \tag{4g}$$

Note that (4b) ensures that the throughput of each BD exceed Q where Q is the slack variable signifying the minimum throughput to be maximized, (4c) ensures the required minimum SINR λ for decoding each BD's signal successfully, (4d) is the required minimum energy E_{min} constraint, (4e) is the constraint for each power reflection coefficient, (4f) and (4g) is the normalization constraint and non-negative constraint for the slot time durations.

III. Optimal Solution

Problem (P1) is a non-convex optimization problem, since both the constraint functions in (4b) and (4d) are not jointly convex with respect to the coupled variables $\boldsymbol{\tau}$ and $\mathbf{\Omega}$. Hence in this letter, we aim to obtain an efficient sub-optimal solution to (P1) by exploiting the block coordinate decent (BCD) technique [16] to solve $\boldsymbol{\tau}$ and $\mathbf{\Omega}$ alternatively. First, for any given power backscatter coefficients $\mathbf{\Omega}^l$ in the *l*-th iteration,

$l \geq 0$, we optimize the $\boldsymbol{\tau}$ by solving the following standard linear program (LP)

$$\text{(P2)}: \max_{\boldsymbol{\tau}, Q} \quad Q \tag{5a}$$

$$\text{s.t.} \quad \tau_k \log_2\left(1+\frac{\rho\|\mathbf{f}_{m,k}\|^4\omega_{m,k}^l}{\sum\limits_{i=m+1}^{M}\rho|\mathbf{f}_{m,k}^H\mathbf{f}_{i,k}|^2\omega_{i,k}^l+\|\mathbf{f}_{m,k}\|^2}\right) \geq Q, \quad \forall m,k \tag{5b}$$

$$\text{(4d)}, \ \text{(4f)}, \ \text{(4g)}. \tag{5c}$$

Second, for given backscatter time allocation $\boldsymbol{\tau}^l$, we optimize the $\boldsymbol{\Omega}$ by solving

$$\text{(P3)}: \max_{\boldsymbol{\Omega}, Q} \quad Q \tag{6a}$$

$$\text{s.t.} \quad \tau_k^l \log_2\left(1+\frac{\rho\|\mathbf{f}_{m,k}\|^4\omega_{m,k}}{\sum\limits_{i=m+1}^{M}\rho|\mathbf{f}_{m,k}^H\mathbf{f}_{i,k}|^2\omega_{i,k}+\|\mathbf{f}_{m,k}\|^2}\right) \geq Q, \quad \forall m,k \tag{6b}$$

$$\text{(4c)}, \ \text{(4d)}, \ \text{(4e)}. \tag{6c}$$

Problem (P3) is non-convex due to the non-convex constraint (6b). However, the successive convex optimization (SCO) technique [17] can be applied to obtain an efficient approximate solution which is guaranteed to converge to at least a locally optimal solution. The basic idea is to successively maximize a lower bound of (P3) in each iteration. The constraint function (6b) can be rewritten as

$$C_{m,k}(\boldsymbol{\Omega}) = \tau_k^l \log_2\left(\sum_{i=m}^{M}\rho|\mathbf{f}_{m,k}^H\mathbf{f}_{i,k}|^2\omega_{i,k}+\|\mathbf{f}_{m,k}\|^2\right) - \tau_k^l \log_2\left(\sum_{i=m+1}^{M}\rho|\mathbf{f}_{m,k}^H\mathbf{f}_{i,k}|^2\omega_{i,k}+\|\mathbf{f}_{m,k}\|^2\right). \tag{7}$$

Notice that the second term $-\tau_k^l \log_2(\cdot)$ in (7) is continuously differentiable and jointly convex with respect to $\omega_{i,k}$, for $i = m+1, \ldots, M$, so it can be globally lower-bounded by its first-order Taylor expansion at any point. Let $\omega_{m,k}^l$ represent the power reflection coefficient in the l th iteration of SCO. We have the following concave lower bound of (6b) at the local point $\omega_{m,k}^l$

$$C_{m,k}(\boldsymbol{\Omega}) \geq \tau_k^l\Bigg[\log_2\left(\sum_{i=m}^{M}\rho|\mathbf{f}_{m,k}^H\mathbf{f}_{i,k}|^2\omega_{i,k}+\|\mathbf{f}_{m,k}\|^2\right) - \log_2\left(\sum_{i=m+1}^{M}\rho|\mathbf{f}_{m,k}^H\mathbf{f}_{i,k}|^2\omega_{i,k}^l+\|\mathbf{f}_{m,k}\|^2\right) - \frac{\rho|\mathbf{f}_{m,k}^H\mathbf{f}_{i,k}|^2(\omega_{m,k}-\omega_{m,k}^l)}{\sum\limits_{i=m+1}^{M}\rho|\mathbf{f}_{m,k}^H\mathbf{f}_{i,k}|^2\omega_{i,k}^l+\|\mathbf{f}_{m,k}\|^2}\Bigg] \triangleq C_{m,k}^{\text{lb}}(\boldsymbol{\Omega}). \tag{8}$$

Algorithm 1 BCD-Based Iterative Algorithm for (P1)

1: Initialize $\boldsymbol{\Omega}^0$. Let $l = 0$ and tolerance $\delta > 0$.
2: **repeat**
3: Solve problem (P2) for given $\boldsymbol{\Omega}^l$, and obtain the solution $\boldsymbol{\tau}^{l+1}$.
4: Solve problem (P4) for given $\boldsymbol{\tau}^{l+1}$ and $\boldsymbol{\Omega}^l$, and obtain the optimal solution as $\boldsymbol{\Omega}^{l+1}$.
5: Update iteration index $l = l + 1$.
6: **until** The fractional increase of the objective value between iterations is smaller than δ.

With the lower bound $C_{m,k}^{\text{lb}}(\boldsymbol{\Omega})$ in (8), by introducing a slack variable Q^{lb}, (P3) is approximated as

$$\text{(P4)}: \max_{\boldsymbol{\Omega}, Q^{\text{lb}}} \quad Q^{\text{lb}} \tag{9a}$$

$$\text{s.t.} \quad C_{m,k}^{\text{lb}}(\boldsymbol{\Omega}) \geq Q^{\text{lb}} \tag{9b}$$

$$\text{(4c)}, \ \text{(4d)}, \ \text{(4e)}. \tag{9c}$$

Problem (P4) is convex and thus can be efficiently solved by existing software tools such as CVX. The lower bound adopted in (9b) implies that the feasible set of (P4) is always a subset of that of (P3). The optimal objective value of (P4) is thus in general a lower bound of that of (P3). The overall algorithm for solving the original problem (P1) is thus obtained by optimizing $\boldsymbol{\tau}$ and $\boldsymbol{\Omega}$ alternately via solving (P2) and (P4) respectively, in an iterative manner, which is summarized in Algorithm 1.

Remark 1: Problem (P1) can also be solved by an alternatively iterative algorithm where the outer-layer iteration updates $\boldsymbol{\tau}$ and $\boldsymbol{\Omega}$ alternately and the update of $\boldsymbol{\Omega}$ is realized by an inner-layer SCO iteration. It can be analytically and numerically shown that the proposed Algorithm 1 is equivalently to this two-layer iterative algorithm but has lower complexity, thus is adopted herein.

The convergence of BCD algorithms requires that each subproblem for optimizing one block of variables should be solved exactly with optimality in each iteration [16]. However, in step 4 of the proposed Algorithm 1, we just solve the approximate problem (P4) optimally to update $\boldsymbol{\Omega}$, instead of the original subproblem (P3). Fortunately, by following similar steps to prove [18, Th. 2], it can be shown that the proposed Algorithm 1 is guaranteed to converge. The reason is twofold. First, the objective value is always non-decreasing after each iteration, although an approximated problem (P4) is solved to obtain a lower-bound objective value of (P3). Second, the objective value of (P1) is upper-bounded by some finite positive number.

IV. Numerical Results

We assume independent Rayleigh fading channels and channel pathloss model $10^{-3}d^{-3}$, where d is the distance with unit of meter (m). We consider four BDs with $M = 2$ and $K = 2$. As in [3] and [11], we set $\sigma^2 = -114$ dBm, $\lambda = 5$ dB, and $\epsilon_{m,k} = \epsilon = 0.5$. Let $R = 4$ and $\delta = 10^{-5}$. The CT-to-BR distance is 12 m. The CT-to-BD and BD-to-BR distance pairs are (4, 10), (8, 18), (5, 13) and (7,15) for BD 1, 2, 3 and 4,

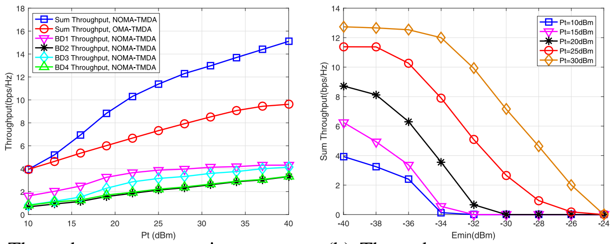

(a) Throughput v.s. transmit power (b) Throughput v.s. energy

Fig. 2. Throughput performance comparison.

respectively. The BDs adopt the instantaneous-channel-power-based dynamic head-tail pairing scheme, which was proved to be optimal for max-min rate optimization in uplink 2-user NOMA (see [12, Th. 4]). The results are based on 1000 channel realizations. For comparison, we consider a benchmark scheme of traditional OMA-TDMA, in which the four BDs individually backscatter signals to the BR in four orthogonal slots and the slot durations are optimized to maximize the minimum throughput among all BDs.

Fig. 2 (a) compares the throughput for the proposed dynamic NOMA-TDMA scheme and the benchmark OMA-TDMA scheme. Let $E_{\min} = 10^{-7}$ Joule (J). We observe that the proposed scheme achieves significant sum-throughput gain compared to the benchmark scheme. The gain in general comes from the radio-resource sharing in NOMA systems, i.e., the proposed scheme allows two BDs to access the BR at the same time, which doubles the time resource each BD can be allocated. We further observe that larger throughput-gain is achieved for higher CT transmit power P_t. This is because that the SINR in the logarithm part of (3) is a monotonically increasing function of ρ (i.e., P_t), leading to higher probability to satisfy the SINR constraints as well as higher rate for decoding the corresponding data stream. Moreover, the BD 2 and BD 4, which have weaker (average) backscatter-link channel strength, achieve almost the same throughput which is comparable to those of BD 1 and BD 3 with stronger channels. This verifies that the proposed scheme achieves better throughput fairness among all BDs. Fig. 2 (b) plots the sum throughput versus the harvested-energy requirement $E_{\min}$ in decibel normalized to 1 millijoule (mJ). There is a tradeoff between the sum throughput and $E_{\min}$, and higher sum-throughput is achieved for higher CT transmit power P_t.

V. Conclusion

This letter has studied the problem of resource allocation in a NOMA-enhanced bistatic backscatter communication network. The BDs' backscatter time allocation and power reflection coefficients are jointly optimized to maximize the minimum throughput among all BDs while ensuring sufficient harvested energy and SINR for NOMA decoding. By utilizing the block coordinated decent and successive convex optimization techniques, an efficient iterative algorithm is proposed to find a sub-optimal solution to the formulated non-convex problem. This design framework can be further extended to the scenario of multiple CTs and multiple BRs for large-scale IoT, where the co-channel interference should be taken into account.

References

[1] A. Bletsas, P. N. Alevizos, and G. Vougioukas, "The art of signal processing in backscatter radio for μw (or less) Internet of Things: Intelligent signal processing and backscatter radio enabling batteryless connectivity," *IEEE Signal Process. Mag.*, vol. 35, no. 5, pp. 28–40, Sep. 2018.

[2] J. Kimionis, A. Bletsas, and J. N. Sahalos, "Increased range bistatic scatter radio," *IEEE Trans. Commun.*, vol. 62, no. 3, pp. 1091–1104, Mar. 2014.

[3] G. Yang, C. K. Ho, and Y. L. Guan, "Multi-antenna wireless energy transfer for backscatter communication systems," *IEEE J. Sel. Areas Commun.*, vol. 33, no. 12, pp. 2974–2987, Dec. 2015.

[4] G. Yang, Y.-C. Liang, R. Zhang, and Y. Pei, "Modulation in the air: Backscatter communication over ambient OFDM carrier," *IEEE Trans. Commun.*, vol. 66, no. 3, pp. 1219–1233, Mar. 2018.

[5] Q. Zhang, H. Guo, Y.-C. Liang, and X. Yuan, "Constellation learning-based signal detection for ambient backscatter communication systems," *IEEE J. Sel. Areas Commun.*, vol. 37, no. 2, pp. 452–463, Feb. 2019.

[6] Y. Liu, Z. Qin, M. Elkashlan, Z. Ding, A. Nallanathan, and L. Hanzo, "Nonorthogonal multiple access for 5G and beyond," *Proc. IEEE*, vol. 105, no. 12, pp. 2347–2381, Dec. 2017.

[7] Q. Zhang, L. Zhang, Y.-C. Liang, and P.-Y. Kam, "Backscatter-NOMA: A symbiotic system of cellular and Internet-of-Things networks," *IEEE Access*, vol. 7, pp. 20000–20013, 2019.

[8] G. Yang, Q. Zhang, and Y.-C. Liang, "Cooperative ambient backscatter communications for green Internet-of-Things," *IEEE Internet Things J.*, vol. 5, no. 2, pp. 1116–1130, Apr. 2018.

[9] R. Long, H. Guo, L. Zhang, and Y.-C. Liang, "Full-duplex backscatter communications in symbiotic radio systems," *IEEE Access*, vol. 7, pp. 21597–21608, 2019.

[10] Y.-C. Liang, R. Long, Q. Zhang, J. Chen, H. V. Cheng, and H. Guo, "Large intelligent surface/antennas (LISA): Making reflective radios smart," *J. Commun. Inf. Netw.*, vol. 4, no. 2, pp. 40–50, Jun. 2019.

[11] J. Guo, X. Zhou, S. Durrani, and H. Yanikomeroglu, "Design of non-orthogonal multiple access enhanced backscatter communication," *IEEE Trans. Wireless Commun.*, vol. 17, no. 10, pp. 6837–6852, Oct. 2018.

[12] M. A. Sedaghat and R. R. Müller, "On user pairing in uplink NOMA," *IEEE Trans. Wireless Commun.*, vol. 17, no. 5, pp. 3474–3486, May 2018.

[13] M. S. Ali, H. Tabassum, and E. Hossain, "Dynamic user clustering and power allocation for uplink and downlink non-orthogonal multiple access (NOMA) systems," *IEEE Access*, vol. 4, pp. 6325–6343, 2016.

[14] C. Boyer and S. Roy, "Backscatter communication and RFID: Coding, energy, and MIMO analysis," *IEEE Trans. Commun.*, vol. 62, no. 3, pp. 770–785, Mar. 2014.

[15] R. Correia, A. Boaventura, and N. B. Carvalho, "Quadrature amplitude backscatter modulator for passive wireless sensors in IoT applications," *IEEE Trans. Microw. Theory Techn.*, vol. 65, no. 4, pp. 1103–1110, Apr. 2017.

[16] M. Hong, M. Razaviyayn, Z.-Q. Luo, and J.-S. Pang, "A unified algorithmic framework for block-structured optimization involving big data: With applications in machine learning and signal processing," *IEEE Signal Process. Mag.*, vol. 33, no. 1, pp. 57–77, Jan. 2016.

[17] A. Beck, A. Ben-Tal, and L. Tetruashvili, "A sequential parametric convex approximation method with applications to nonconvex truss topology design problems," *J. Glob. Optim.*, vol. 47, no. 1, pp. 29–51, May 2010.

[18] G. Yang, D. Yuan, Y.-C. Liang, R. Zhang, and V. C. M. Leung, "Optimal resource allocation in full-duplex ambient backscatter communication networks for wireless-powered IoT," *IEEE Internet Things J.*, vol. 6, no. 2, pp. 2612–2625, Apr. 2019.